Solar Energy Materials & Solar Cells 157 (2016) 415–421

Contents lists available at ScienceDirect

Solar Energy Materials & Solar Cells

journal homepage: www.elsevier.com/locate/solmat

Comparative analysis of upconversion efficiencies in fluoride materials for photovoltaic application

Elena Favilla [b,*], Giovanni Cittadino [a], Stefano Veronesi [b], Mauro Tonelli [b], Stefan Fischer [c], Jan Christoph Goldschmidt [c], Arlete Cassanho [d], Hans P. Jenssen [e]

[a] Dipartimento di Fisica, Universita' di Pisa, Largo B. Pontecorvo 3, I-56127 Pisa, Italy
[b] NEST Istituto Nanoscienze-CNR Pisa, Piazza San Silvestro 12, 56127 Pisa, Italy and Dipartimento di Fisica dell'Università di Pisa, Largo B. Pontecorvo 3, Pisa, Italy
[c] Fraunhofer Institute for Solar Energy Systems ISE, Heidenhofstrasse 2, 79110 Freiburg, Germany
[d] AC Materials, Inc., 756 Anclote Road, Tarpon Springs, FL 34689, USA
[e] CREOL, The College of Optics and Photonics, University of Central Florida, 4000 Central Florida Boulevard, Orlando, FL 32816, USA

ARTICLE INFO

Article history:
Received 23 October 2015
Received in revised form
28 April 2016
Accepted 2 May 2016
Available online 18 July 2016

Keywords:
Photovoltaics
Bifacial silicon solar cells
Upconversion
Fluorides
Monocrystals
Photoluminescence

ABSTRACT

Infrared to visible upconversion (UC) is a promising way to enhance the efficiency of silicon based solar cells. In this paper, the spectral conversion and recovery of sub-band gap photons of the solar spectrum, from NIR-IR to the VIS-NIR wavelength region, is investigated in two fluorides hosts doped with trivalent erbium ions (Er^{3+}). The efficiency gain due to upconversion in silicon solar cells is compared for single crystal samples of BaY_2F_8:Er^{3+} and $LiYF_4$:Er^{3+} in a dedicated upconverter solar cell device (UCSCD) with monochromatic excitation in the 1.5 μm spectral region.

The highest external quantum efficiency due to upconversion was found for the UCSCD using the BaY_2F_8:30 at% Er^{3+} single crystal, reaching an EQE of $6.8 \pm 0.2\%$ for $(1.10 \pm 0.12) \cdot 10^5$ W m^{-2} spectral irradiance at 1494 nm.

We present a comprehensive spectroscopic study of the crystal samples also taking into account the effects of the different crystal symmetry as well as the different phonon energies. Our findings enable us to explain the higher efficiency of the BaY_2F_8:Er^{3+} compared to the $LiYF_4$:Er^{3+} upconverter in terms of both static and dynamic properties.

1. Introduction

One of the most important limiting factors for the efficiency of a solar cell is related to photons with energy below the band gap of the solar cell material, which are not utilized. This low energy part of the solar spectrum can be accessed using upconversion processes where two or more incoming photons, interacting with the upconverter, are transformed in one photon having an energy that is higher than the single incoming photon one.

The upconverting property of rare earth (RE) materials is widely used in many applications such as solid state lasers [1], light emitting devices like infrared indicator cards, bio-labels [2] or for three-dimensional displays [3].

Among the possible upconverters to be used with silicon solar cells, erbium is one of the most promising due to the $^4I_{15/2} \rightarrow {}^4I_{13/2}$ ground state absorption around 1500 nm and emissions in the green (~540 nm), red (~650 nm) and NIR (~980 nm), within the useful range for this kind of solar cell (see Fig. 1). In fact, the dominant emission at 980 nm can be efficiently used by a silicon solar cell. The pioneering studies of this approach were performed using sodium yttrium fluoride ($NaYF_4$). It has been successfully applied as upconverter in the hexagonal form (β-$NaYF_4$), doped with trivalent erbium ions (Er^{3+}) on the rear side of a bifacial silicon solar cell as reported by Shalav et al. [4,5] and Fischer et al. [6]. In addition to $NaYF_4$, gadolinium oxysulfide (Gd_2O_2S) host lattice doped with erbium has been studied intensively [7–12]. It shows an intense UC luminescence and it has demonstrated to be a good converter in biological imaging application, where a monochromatic excitation is needed, while for silicon solar cells, where a broader excitation spectrum is present, β-$NaYF_4$:25 at% Er^{3+} powders showed a better performance as upconverter [13]. More recently upconverter solar cell devices (UCSCDs) with β-$NaYF_4$:25 at% Er^{3+} have shown a relative enhancement of 0.16% in the short-circuit current under broad band excitation ranging from 1450 to 1600 nm with a correspondent EQE of 1.28% for an irradiance of 2570 W m^{-2} [14]. A relative increase in the solar cell's efficiency of 0.19% was reported for illumination from a solar

* Corresponding author.

http://dx.doi.org/10.1016/j.solmat.2016.05.005
0927-0248/

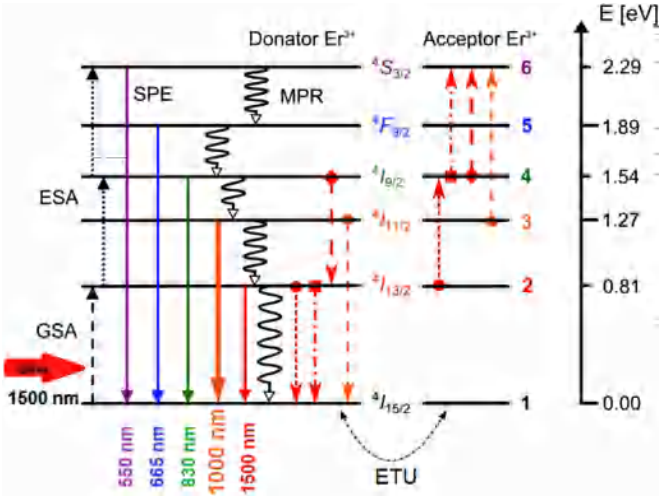

Fig. 1. Energy level diagram of Er^{3+}, depicting the five lowest energy levels and the most important processes involved in the upconversion. These are especially ground state absorption (GSA), energy transfer upconversion (ETU), multi-phonon relaxation (MPR) and spontaneous emission (SPE).

simulator, where the light was concentrated with a lens by a factor of 210 [13].

Because of its good performance relative to other upconverter materials, up to now most of the work concerning PV-UC applications was done using β-$NaYF_4$ microcrystalline powders doped with erbium as upconverter. However, the achieved enhancements of the solar cell efficiency are still not sufficient for a wide-spread application of upconversion in photovoltaic. Consequently there is a need for exploring new materials that are able to significantly enhance the total efficiency of photovoltaic devices. The family of fluorides, due to their favourable optical properties both as single crystals or microcrystalline powders, is a promising area to search candidates for this application.

Due to a stronger Stark splitting, doped fluorides show excitation bands much broader than other host materials such as chlorides [15]. Hence they absorb a larger fraction of the incident solar spectrum. A key point for the efficiency of the UC process is related to phonon energy which strongly influences the performances by non-radiative losses, especially due to multiphonon decay. Therefore, the phonon cut off energy of the medium plays a vital role: higher phonon energy leads to a higher rate of non-radiative transitions and typically to a lower UC efficiency. Due to their low phonon energy, most fluoride crystals are attractive hosts to realize upconverters based on RE trivalent ions. Furthermore, their good thermo-mechanical and chemical properties guarantee their durability, small aging effects, and they allow a large doping concentration which consequently leads to strong absorption of the incident light. Furthermore, large doping results in small average distances between the RE ions, which enhances energy transfer processes, such as energy transfer upconversion (ETU), and therefore increases the upconversion quantum yield at least for the low irradiance conditions that are relevant in photovoltaic applications. However, for very high RE doping the UCQY decreases due to concentration quenching. The optimal concentration is a result of balance between the beneficial ETU processes and the concentration quenching for high RE doping, which also depends on the irradiance of the excitation [11].

One fluoride host material which is a good alternative to β-$NaYF_4$ is BaY_2F_8. BaY_2F_8 was used already in a preliminary work on a PV-UC device with a monofacial silicon cell [16] and showed a potential EQE comparable to the "reference" β-$NaYF_4$ materials used for this type of application. In another work, BaY_2F_8 showed that it can even outperform β-$NaYF_4$ as a host material for erbium as upconverter in photovoltaic applications. Indeed, at an illumination with a solar simulator and solar concentration of 94 ± 17 suns, the upconverter solar cell device using a BaY_2F_8:30 at% Er^{3+} sample showed a record relative enhancement of the short-circuit current of $0.55 \pm 0.14\%$ [17]. Another, yet unexplored option is $LiYF_4$. This crystalline host is a very well-known material that is often used as a reference in laser sources development, because of its good thermo-mechanical properties, low phonon energies and negative dn/dT benefiting low thermal lensing [18]. It is at present widely used in commercial devices (even operating at high power), and it has been used as an active laser medium doped with almost all rare earth ions. However, it has only rarely been used in photovoltaic [19] and no good quantitative data exists.

In this paper, we report a comparison of two fluoride hosts, the current champion material single crystalline BaY_2F_8 with the new option of single crystalline $LiYF_4$, for the application in photovoltaics. Samples were realized from high optical quality crystal boules grown with the Czochralski technique. The single-crystal samples of BaY_2F_8:30 at% Er^{3+} were attached to the rear side of a planar bifacial silicon solar cell that features broad-band anti-reflection coatings and was optimized for the UC application [20]. The effect of reabsorption by the crystal was evaluated to achieve the best performances, by utilizing several thicknesses correspondent to different absorbed pumping powers. The results are then compared with those for $LiYF_4$ single crystal doped with 25 at% Er^{3+}. Our results show the appealing performances of these materials to realize innovative photovoltaic devices.

2. Material and methods

2.1. Upconverter materials

In this work, we explored and compared two materials as upconverter for silicon solar cell devices: BaY_2F_8 (BYF in the following) doped with 30 at% Er^{3+} and $LiYF_4$ (YLF in the following) doped with 25 at% Er^{3+}. The Er:BYF single crystal was grown in a homemade furnace with conventional resistive heating and automatic optical diameter-control. All the raw powders utilized in the growth, having 5 N purity, were provided by AC Materials (Tarpon Springs, FL, USA). The chosen doping concentration was achieved by adding a proper amount of ErF_3 and of BaF_2 to the BaY_2F_8 powders [21].

The BYF host lattice has a monoclinic structure belonging to the space group C2/m, each primitive cell has two molecules while lattice constants are $a=6.972$ Å, $b=10.505$ Å, $c=4.260$ Å, and angles between crystallographic axes are $\alpha=90°$, $\beta=90°$ and $\gamma=99.76°$. Additionally, it has a refractive index $n \cong 1.5$ and low phonon energy ($\cong 350\ cm^{-1}$) [22]. The monoclinic structure is an important feature of this crystal because it introduces a low symmetry structure, which leads to wider absorption and emission bandwidths.

The Er:YLF single crystal was provided by AC Materials (Tarpon Springs, FL, USA).

$LiYF_4$ is an uniaxial crystal with a tetragonal structure belonging to the Scheelite ($CaWO_4$) family and having C64h (I41/a) space group. The primitive cell has four molecules and its dimensions are: $a=b=5.160$ Å, $c=10.85$ Å [23]; rare earth ions substitute Y^{3+}, in a site having point symmetry S4. Its transparency region extends from the visible up to infrared (5 μm). It has a refractive index $n \cong 1.5$.

The structural investigation on the boules by X-ray Laue technique allowed for identifying the crystallographic axes of the crystals and confirms the single crystal character of the boules. Moreover an optical analysis with a laser beam probe confirmed

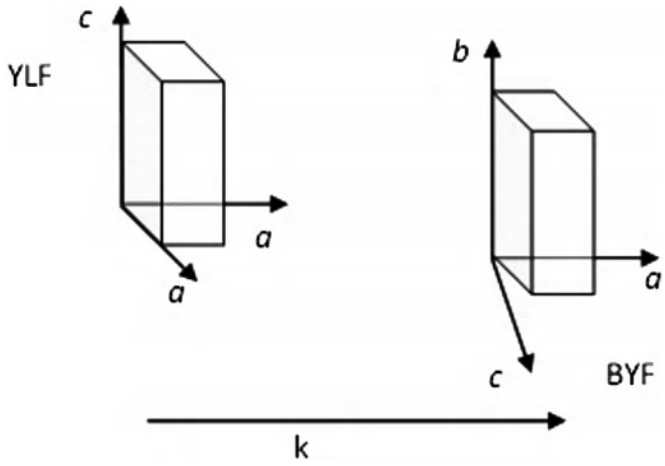

Fig. 2. Schematic picture of the crystal samples with crystallographic axes and the k vector orientation of the illumination. The angle between *a* and *c* axis is 99.76°.

that the crystals were of high optical quality free of cracks and micro-bubbles.

2.2. Optical characterization: experimental set-ups

2.2.1. Absorption

Absorption measurements at room temperature were collected with a Cary 500 Varian spectrophotometer. Unpolarized absorption spectra were recorded in the region between 200 and 1700 nm, with a resolution of 0.3 nm in the UV–vis range (200–830 nm), and with a resolution of 0.5 nm in the near IR range (830–1700 nm). The samples orientation in the absorption measurement, as well as in the UCSCD, were in such a way that the crystallographic *a* axis of YLF samples and the *k*-vector of the illumination light were parallel, while the plane perpendicular to the propagation of light contains the *b* axis for the BYF samples and *c*-*a* axes for YLF ones. A sketch of the samples with crystallographic axes orientation and *k* propagation vector is shown in Fig. 2.

2.2.2. Fluorescence

The fluorescence measurement was done in the same conditions of illumination (same excitation laser and same upconverter samples) as the ones adopted for the UCSCD. The fluorescence in the VIS and NIR wavelength range was collected after optimization of the NIR emission intensity by laser focusing adjustments on each sample. In this way we are confident to reproduce the same illumination and emission state of the upconverter crystals as in the EQE measurements. In that case, the laser focusing was adjusted to maximise the current signal (originating mainly from the NIR converted emission, for which the solar cell back side has the higher EQE as reported in the following).

The fluorescence from the upconverter crystal samples excited by the laser at 1494 nm was collected using the experimental set up described in Fig. 3. The crystal samples were mounted inside a 150 mm diameter integrating sphere and mounted on a sample holder coated with $BaSO_4$. The excitation laser beam propagating perpendicular to the collecting direction was focused by an f=200 mm focal length lens. Due to the large sphere diameter the laser was focused on the samples with a longer focal length lens than that one used to focus on the UCSCD. The fluorescence signal was collected by a fibre Spectrometer model QEpro Ocean Optics and acquired by a PC and relative software. The fluorescence spectra were acquired in the range 350–1100 nm with a 0.8 nm resolution and they were normalized for the optical response of the optical system using an Ocean Optics HL-3***plus***-INT-CAL calibrated lamp.

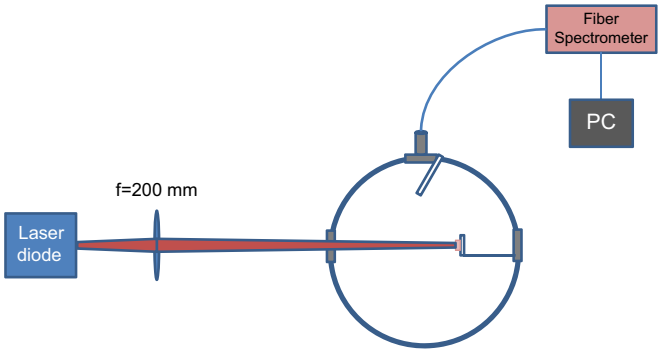

Fig. 3. Scheme of the experimental set up used for fluorescence measurements on the upconverter crystal samples. The scheme is intended to reproduce the experimental conditions (excitation of the UC crystal and detection of the fluorescence signal impinging on the back side of the PV cell) in the UCSCD.

2.2.3. Lifetime

The fluorescence decay time of the levels $^4S_{3/2}$ and $^4F_{9/2}$, involved in the upconversion processes, was obtained by exciting at 486 nm with a frequency doubled titanium sapphire pulsed laser, using a BBO nonlinear crystal. Pulse duration was 30 ns, and repetition rate 10 Hz. The fluorescence decay time of the level $^4I_{11/2}$ was acquired exciting in band at 965 nm using the beam extracted from the TiSa pulsed laser and collecting the fluorescence at 1010 nm so to remove as much as possible the spurious signal from the exciting laser radiation. The intrinsic fluorescence lifetime was extrapolated using the pinhole method [24]. The fluorescence decay time for $^4I_{13/2}$ manifold was obtained by exploiting the laser diode tuned to 1494 nm. For these measurements the laser beam was modulated by a chopper which allows a pulse duration of 100 ms and a repetition rate of 5 Hz. Independently on pumping method, the exciting beam has been focused on the samples utilizing appropriate optics. The time dependent signal was analyzed by a monochromator Triax 320 and detected by phototube in the visible range or an indium antimonide (InSb) detector in the IR range and finally acquired through an oscilloscope connected to a PC.

2.3. Application of the two crystals to a bifacial cell for a UCSCD device

Upconverter samples for the PV-UC device were parallelepipeds of aperture 4×4 mm^2 having different thicknesses, cut and polished to optical grade.

The PV-UC device was realized using a bifacial silicon solar cell that features a double-layer anti-reflection coating (ARC) on the front optimized for high broad-band transmittance of sub-band gap photons (81% measured transmission at 1494 nm). The rear surface features a single layer ARC designed for high transmission of sub-band gap photons and low reflectivity and high quantum efficiency for photons emitted by the upconverter at 980 nm with an EQE value of 86% [25].

The PV-UC device scheme used in this work is shown in Fig. 4. The upconverter sample was put behind the cell and kept at a distance of roughly 0.1 mm from the back surface of the cell by using a micrometric translator. A $BaSO_4$ substrate was used as back reflector behind the sample.

The experimental set up used to measure the external quantum efficiency of the PV-UC device is basically the same as that reported in [16]. The incident power is measured collecting, on an InGaAs photodiode, the reflected beam from a wedged window. The detector calibration is performed relating its output signal with the power incident on the PV-UC device, measured with an Ophir power meter head. After the wedged windows the laser beam is focused on the solar cell with a 4 cm focal length lens. The

PV-UC device is connected to a digital ammeter for the measurement of the short-circuit current. The signal has been optimized moving the upconverter.

The irradiance has been calculated from the laser spot area A= $(1.4 \pm 0.1) \cdot 10^{-3}$ cm^2, determined in the solar cell position from a 10/90% knife edge method.

3. Results and discussion

3.1. Optical characterization: results

A RTL 1500-30G laser diode was used as excitation source which was tuned to 1494 nm for photoluminescence and the device measurements. This wavelength belongs to the spectral region were both crystals have a high absorption coefficient corresponding to α=45.6 cm^{-1} and α=44.0 cm^{-1} for the BYF and YLF crystal respectively.

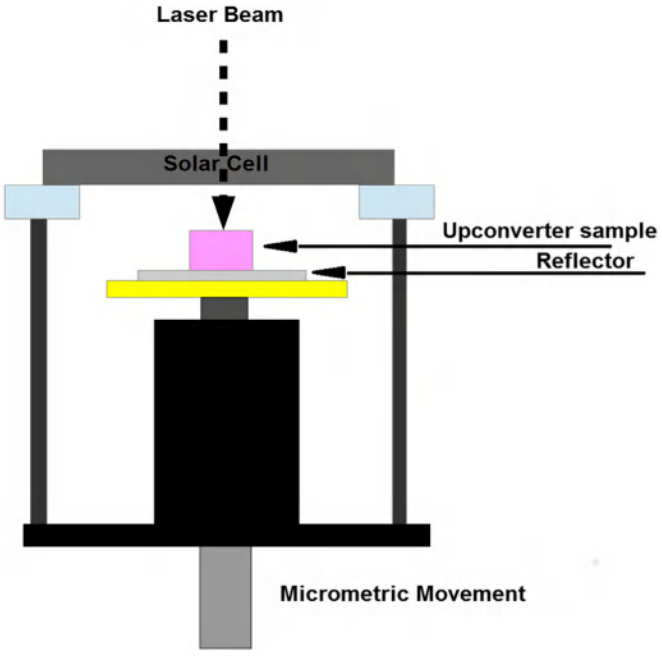

Fig. 4. Sketch of the PV-UC device. The black parts are made of anodized brass and the yellow disc is uncoated brass. The emission light directly impinging on these two parts can be considered negligible.

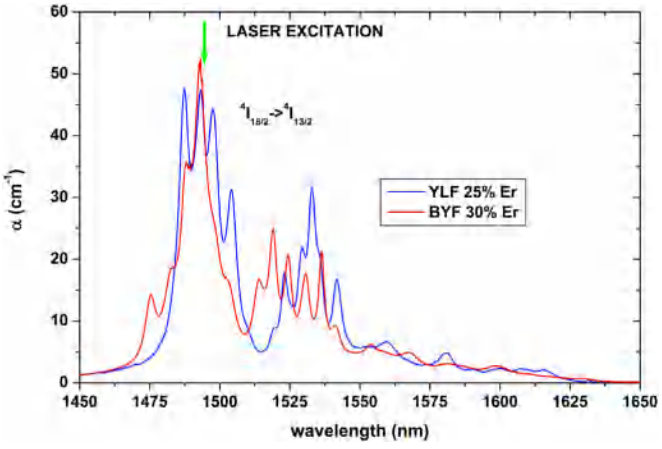

Fig. 5. Absorption spectra of BYF30%Er and YLF: 25%Er crystals in the 1450–1650 nm interval.

Fig. 5 shows the absorption spectra of Er:BYF and Er:YLF crystals in the range 1450–1650 nm corresponding to the transition from the ground state $^4I_{15/2}$ to the first excited manifolds $^4I_{13/2}$ of erbium. The arrow indicates the laser excitation wavelength used for the PV-UC experiments.

Emission spectra recorded at room temperature upon 1494 nm excitation of the two crystals zoomed in the 500–1100 nm wavelength interval is shown in Fig. 6. The spectra were recorded for (14.7 ± 0.6) mW incident power corresponding to the maximum power incident on the samples in the UCSCD.

Comparing the normalized fluorescence ratio in the visible (500–900 nm) and in the NIR (900–1100 nm) wavelength intervals for both crystals we find that most (around 99%) of the emission is due to the $^4I_{11/2} \rightarrow {}^4I_{15/2}$ transition around 1 μm for both host materials.

This is a signature of the upconversion mechanism which populates higher erbium manifolds in particular, with a two photons process, the $^4I_{11/2}$ corresponding to the 980 nm emission and the $^4F_{9/2}$ and $^4S_{3/2}$ with a three/four photons processes. For a more detailed description of the dynamics of the population processes the reader should refer to [16]. Comparing the spectra of the two crystals in the 900–1100 nm interval we obtain an emission yield of the BYF sample which is 2 higher than the YLF one. Taking into account the very close values of the absorption coefficient of the two crystals at the pumping wavelength and that the samples are excited with the same incident power this is a mark of the better conversion at 1 μm of the exciting radiation for the BYF sample.

The spectroscopic analysis performed so far does not describe completely the aspects which influence the upconversion processes. Manifolds lifetime should in fact be taken into account. To

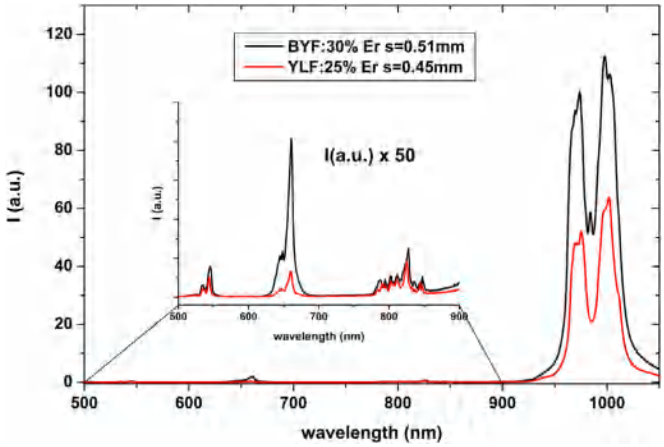

Fig. 6. Fluorescence spectra of the BYF: 30% Er and YLF: 25% Er upconverter samples adopted for the PV-UC device in the 500–1100 nm wavelength interval following laser excitation at 1494 nm. The two shown spectra were recorded in the same conditions of illumination and are normalized for the optical response of the measurement system.

Table 1
Fluorescence decay time values were evaluated under excitation at 486 nm for $^4S_{3/2}$ and $^4F_{9/2}$ manifolds, excitation at 965 nm for $^4I_{11/2}$ and excitation at 1494 nm for $^4I_{13/2}$ manifold respectively. The $^4I_{11/2}$ decay time reported here was extrapolated by the pinhole method.

BYF:30 at%Er	**$^4S_{3/2}$**	**$^4F_{9/2}$**	**$^4I_{11/2}$**	**$^4I_{13/2}$**
τ[a]	5.8 ± 0.1 μs	398 ± 2 μs	10.4 ± 0.3 ms	15.8 ± 0.6 ms
YLF:25 at%Er	**$^4S_{3/2}$**	**$^4F_{9/2}$**	**$^4I_{11/2}$**	**$^4I_{13/2}$**
τ[a]	5.7 ± 0.1 μs	64.0 ± 0.6 μs	5.3 ± 0.6 ms	14.2 ± 0.1 ms

[a] Errors originate from the statistic of the fitting procedure.

exploit this aspect, decay time of the fluorescence emission from the $^4S_{3/2}$, $^4F_{9/2}$, $^4I_{11/2}$ and $^4I_{13/2}$ erbium manifolds were measured in both crystal hosts.

In Table 1 we report the fluorescence decay time of the levels $^4S_{3/2}$, $^4F_{9/2}$, $^4I_{11/2}$ and $^4I_{13/2}$ obtained from exponential decay fits of the fluorescence signals acquired for both host materials.

The concentration quenching becomes very important for these so high doping concentrations and is responsible of the reduced decay time of the $^4S_{3/2}$ in agreement with the behaviour reported in [26] for BYF and YLF and in [27] for CaF_2 hosts. There are less literature data for $^4F_{9/2}$ level, but at low concentration the lifetime in BYF is about 7 times longer than in YLF [26]. The $^4I_{13/2}$ measured fluorescence decay time both in BYF and YLF crystal hosts are comparable with values reported in literature [28] for other fluoride hosts.

As we are considering transitions to the ground state the effect of reabsorption is very strong. In order to suppress reabsorption artifacts in $^4I_{11/2}$ lifetime measurement we measured the lifetime of this level exciting at 965 nm using the pinhole method [24]. A value of 10.4 ms for BYF and 5.8 ms for YLF has been extrapolated. The probability of ETU mechanisms is proportional to the product of the starting levels ($^4I_{13/2}$, $^4I_{11/2}$) populations so ETU benefits of longer level lifetime that ensures a larger level population for longer time. Hence, the longer lifetime of this manifold in BYF could be responsible of the increased efficiency of the second order upconversion process ($^4I_{13/2}$, $^4I_{11/2}$) → ($^4F_{9/2}$, $^4I_{15/2}$) leading to the longer $^4F_{9/2}$ lifetime measured in BYF than in YLF. This was confirmed also by fluorescence measurements in which we find a preponderance of signal in the red wavelength region compared to the green signal.

The value obtained for the $^4I_{11/2}$ level is comparable in YLF for similar doping concentrations [26]. As is evident from Table 1, the $^4I_{11/2}$ lifetime found in BYF is about two times longer than in YLF. A much longer fluorescence in BYF than in YLF has already been found in [26] for 10% doping concentration.

3.2. EQE measurements

The EQE, defined as the ratio between the number of electrons collected by the solar cell and the number of incident photons, was determined using the relation:

$$EQE = \frac{hc}{e\lambda_{laser}} \frac{I_{sc}}{P_{inc}}$$

Where I_{sc} is the measured short-circuit current and P_{inc} the incident optical power measured as previously described.

A common parameter used to characterize the efficiency of a PV device is the normalized EQE (NEQE), which corresponds to the EQE divided by the irradiance. Even if the aim of this work is not to compare our results on UCPV device with others but only to compare different UC materials behaviour in a PV device, we will give also results in terms of NEQE.

The PV-UC device using Er:BYF or Er:YLF crystals as upconverters was tested with laser excitation at 1494 nm. The EQE was measured as function of both the incident power and the upconverter sample thickness. Indeed, the resultant EQE of the device depends on the best compromise between absorbed pump power, from which the upconversion process originates, and the fraction of the converted power emitted at 1 μm not reabsorbed by the crystal.

Table 2
Absorbed percentage of laser power at 1494 nm and relative UC samples thicknesses. All the samples were parallelepipeds of aperture 4 × 4 mm².

Host	Sample thickness (mm)	Absorbed pump power (%)
YLF	1.10	96
	0.45	86
	0.31	74
BYF	0.91	94
	0.51	86

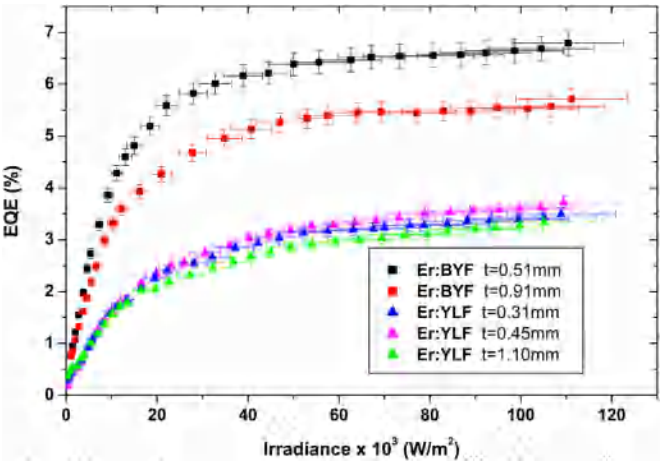

Fig. 7. EQE (%) of BYF: 30%Er and YLF: 25% Er crystal PV-UC devices as a function of the 1494 nm cw laser excitation irradiance and of sample thickness.

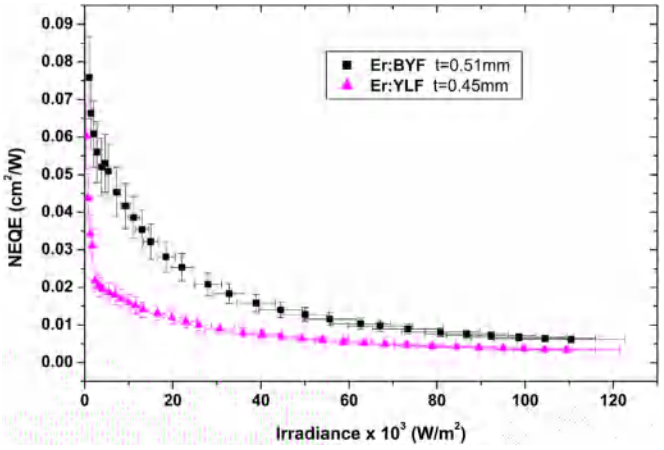

Fig. 8. Normalized EQE (cm²/W) with the best performance BYF and YLF samples, BYF: 30% Er 0.51 mm thickness sample and YLF: 25% Er 0.45 mm thickness, as a function of the 1494 nm laser irradiance.

All the measurements show saturation in the EQE curve as the irradiance increases, which is due to competitive processes like concentration quenching or higher order processes. Accordingly, contrary to the EQE, the higher normalized EQE values are found, as usual in a UCPV device, for lower irradiances [17].

The highest EQE value of $6.8 \pm 0.2\%$ was reached using $(1.10 \pm 0.12) \cdot 10^5$ W m^{-2} at 1494 nm laser radiation with the 0.51 mm thick Er:BYF upconverter sample corresponding to a normalized value (NEQE) of 0.0062 ± 0.0009 cm²/W (see Fig. 8). The highest NEQE value found was 0.076 ± 0.011 cm²/W at irradiation of $(1.00 \pm 0.11) \cdot 10^3$ W m^{-2} at 1494 nm. The same material has been previously used in UCSCD and gave a NEQE of 0.177 against 0.053 in this work at irradiance values close to $4.5 \cdot 10^3$ W m^{-2} [17].

Furthermore, we estimated the potential current gain, which could be achieved under illumination with the AM1.5g solar spectrum. For this purpose, we assumed that the EQE(λ) is proportional to the absorption derived by the Lambert-Beer law from the displayed absorption coefficient. Following the definitions in [14], we calculated equivalent concentration factors, which tell how much the solar illumination has to be concentrated in order to achieve the same amount of absorbed photons as under the monochromatic illumination. For the best Er:BYF upconverter sample, the $(1.10 \pm 0.12) \cdot 10^5\ \mathrm{W\,m^{-2}}$ irradiance at 1494 nm corresponds to a concentration factor of 8583x, for the Er:YLF sample, a similar concentration factor of 8602x was determined (the differences originate from the slightly different absorption spectra). By integrating over the product of estimated EQE(λ) and the concentrated photon flux in the spectral range from 1450 to 1650 nm, we estimated an increase in short-circuit current density due to upconversion of 732 mA/cm^2 for the Er:BYF and 344 mA/cm^2 for the Er:YLF. Under the assumption that the current of the silicon solar cells scales linearly with the concentration, even at these very high levels, this would correspond to a relative increase of about 0.2% and 0.1%, respectively. This is lower than the 0.55% reported already for a much lower concentration in [17]. This can be attributed partly to the thinner samples being used in this work, which reduces absorption. However, it has not been the purpose of this work this work to achieve highest EQE, but to compare different hosts in the same experimental conditions. This comparison between Er:BYF and Er: YLF samples having similar doping levels and same geometry shows that the BYF host give a better performance with the same UCPV device upon very close irradiance conditions returning an EQE ~50% higher than YLF.

This result is consistent with the spectroscopic analysis made on the two samples reported here, which is in agreement with the better emission efficiency of BYF sample in the 1 μm wavelength region.

3.3. Conclusion and future work

Due to upconversion, the otherwise lost sub-band gap photons can be utilized to enhance the efficiency of photovoltaic devices. In previous studies β-$NaYF_4$ microcrystalline powder doped with erbium was used as upconverter in crystalline silicon based PV-UC device and appreciable efficiency improvement was demonstrated. However, the enhancement of the solar cell's efficiency still remains too low. Consequently, we are aiming to find new materials that are more favourable for solar applications. In this study, we investigated PV-UC devices composed of a bifacial silicon solar cell and single crystals of BaY_2F_8:30 at% Er^{3+} and $LiYF_4$:25 at% Er^{3+} as upconverters.

The EQE was determined under monochromatic laser excitation at 1494 nm for BYF:30 at% Er and for YLF:25 at% Er.

The results, obtained upon laser radiation at 1494 nm, were compared for the PV-UC device using various samples of the two upconverter materials. The highest EQE and NEQE were found for PV-UC device with BYF:30% Er upconverter crystal sample, 0.51 mm thick, achieving $6.8 \pm 0.2\%$ EQE with $(1.10 \pm 0.12) \cdot 10^5\ \mathrm{W\,m^{-2}}$ and $0.076 \pm 0.011\ \mathrm{cm^2/W}$ NEQE with $(1.00 \pm 0.11) \cdot 10^3\ \mathrm{W\,m^{-2}}$. The YLF:25% Er sample 0.45 mm thick achieves the highest EQE of $3.7 \pm 0.1\%$ only, supplying $(1.09 \pm 0.12) \cdot 10^5\ \mathrm{W\,m^{-2}}$ and highest NEQE value of $0.060 \pm 0.009\ \mathrm{cm^2/W}$ with $(0.30 \pm 0.03) \cdot 10^3\ \mathrm{W \cdot m^{-2}}$.

The different outcomes obtained for the two materials in the UCSCD match the results of fluorescence measurements both in static and dynamic domain. The fluorescence spectra highlight the higher emission in the 1 μm wavelength region of BYF crystal than for YLF, benefiting the larger conversion of the 1.5 μm radiation, for which the silicon solar cells are transparent, into the NIR spectral interval were they are very efficient. The higher efficiency of BYF:30% Er as upconverter was confirmed also by measuring the dynamical behaviour of population depletion of the excited level $^4I_{11/2}$ from which the 1 μm emission originates.

These findings corroborate the results obtained in [16] and confirm that BYF:30% Er can be considered a promising material for photovoltaic application. Future work should focus on testing additional materials having not only the monoclinic crystallographic structure, or demonstrating lower symmetry properties of the site which result in a broadening of absorption and emission bands of active ions inside of the host.

Acknowledgement

The Italian group in Pisa would like to acknowledge support from Project “Increased solar energy conversion” ACES (183/2011) of Fondazione Pisa and I. Grassini for the skill and competence in preparing the samples.

References

[1] R. Scheps, Upconversion laser processes, Prog. Quantum. Electron. 20 (1996) 271–358.
[2] R. Niedbala, H. Feindt, K. Kardos, T. Vail, J. Burton, B. Bielska, S. Li, D. Milunic, P. Bourdelle, R. Vallejo, Detection of analytes by immunoassay using up-converting phosphor technology, Anal. Biochem. 293 (2001) 22–30.
[3] E. Downing, L. Hesselink, J. Ralston, R. Macfarlane, A three-color, solid-state, three-dimensional display, Science 273 (1996) 1185–1189.
[4] A. Shalav, B.S. Richards, T. Trupke, R.P. Corkish, K.W. Krämer, H.U. Güdel, M.A. Green, The application of up-converting phosphors for increased solar cell conversion efficiencies, in Proceedings of the 3rd World Conference on Photovoltaic Energy Conversion, 2003 pp. 248–250.
[5] A. Shalav, B.S. Richards, M.A. Green, Luminescent layers for enhanced silicon solar cell performance: Up-conversion, Sol. Energy Mater. Sol. Cells 91 (2007) 829–842.
[6] S. Fischer, J.C. Goldschmidt, P. Löper, G.H. Bauer, R. Brüggemann, K.W. Krämer, D. Biner, M. Hermle, S.W. Glunz, Enhancement of silicon solar cell efficiency by upconversion: optical and electrical characterization, J. Appl. Phys. 108 (2010) 044912.
[7] S. Fischer, R. Martin-Rodriguez, B. Fröhlich, K.W. Krämer, A. Meijerink, J.C. Goldschmidt, Upconversion quantum yield of Er^{3+}-doped β-$NaYF_4$ and Gd_2O_2S: the effects of host lattice, Er^{3+} doping and excitation spectrum bandwidth, J. Lumin. 153 (2014) 281–287.
[8] R. Martin-Rodriguez, F.T. Rabouw, M. Trevisani, M. Bettinelli, A. Meijerink, Upconversion dynamics in Er^{3+}-doped Gd_2O_2S: influence of excitation power, Er^{3+} concentration, and defects, Adv. Opt. Mater. 3 (2015) 558–566.
[9] R. Martin-Rodriguez, S. Fischer, A. Ivaturi, B. Fröhlich, K.W. Krämer, J.C. Goldschmidt, B.S. Richards, A. Meijerink, Highly efficient IR to NIR upconversion in Gd_2O_2S: Er^{3+} for photovoltaic applications, Chem. Mater. 25 (2013) 1912–1921.
[10] M. Pokhrel, G.A. Kumar, D.K. Sardar, Highly efficient NIR to NIR and VIS upconversion in Er^{3+} and Yb^{3+} doped in M_2O_2S (M=Gd, La, Y), J. Mater. Chem. A 1 (2013) 11595–11606.
[11] S. Fischer, B. Fröhlich, K.W. Krämer, J.C. Goldschmidt, Relation between excitation power density and Er^{3+} doping yielding the highest absolute upconversion quantum yield, J. Phys. Chem. C 118 (2014) 30106–30114.
[12] G.A. Kumar, M. Pokhrel, D.K. Sardar, Intense visible and near infrared upconversion in M2O2S: Er (M=Y, Gd, La) phosphor under 1550 nm excitation, Mater. Lett. 68 (2012) 395–398.
[13] S. Fischer, A. Ivaturi, B. Fröhlich, M. Rudiger, A. Richter, K.W. Kramer, B.S. Richards, J.C. Goldschmidt, Upconverter silicon solar cell devices for efficient utilization of sub-band-gap photons under concentrated solar radiation, IEEE J. Photovolt. 4 (2014) 183–189.
[14] S. Fischer, B. Fröhlich, H. Steinkemper, K.W. Krämer, J.C. Goldschmidt, Absolute upconversion quantum yield of β-NaYF 4 doped with Er^{3+} and external quantum efficiency of upconverter solar cell devices under broad-band excitation considering spectral mismatch corrections, Sol. Energy Mater. Sol. Cells 122 (2014) 197–207.
[15] J. Ohwaki, Y. Wang, Efficient 1.5 μm to Visible Upconversion in Er^{3+} doped halide phosphors, Jpn. J. Appl. Phys. 33 (1994) L-334–L337.
[16] A. Boccolini, R. Faoro, E. Favilla, S. Veronesi, M. Tonelli, BaY2F8 doped with Er^{3+}: an upconverter material for photovoltaic application, J. Appl. Phys. 114 (2013) 064904–064904–6.
[17] S. Fischer, E. Favilla, M. Tonelli, J.C. Goldschmidt, Record efficient upconverter solar cell devices with optimized bifacial silicon solar cells and monocrystalline BaYF8:30% Er^{3+} upconverter, Sol. Energy Mater. Sol. Cells 136 (2015) 127–134.

[18] P.J. Hardman, W.A. Clarkson, G.J. Friel, M. Pollnau, D.C. Hanna, Energy-transfer upconversion and thermal lensing in high-power end-pumped Nd:YLF laser crystals, IEEE J. Quantum Electron. 35 (1999) 647–655.
[19] J.C. Goldschmidt, S. Fischer, Upconversion for Photovoltaics – a review of materials, devices and concepts for performance enhancement, Adv. Opt. Mater. 3 (2015) 510–535.
[20] M. Rüdiger, C. Schmiga, M. Rauer, M. Hermle, S.W. Glunz, Optimisation of industrial n-type silicon solar cells with aluminium-alloyed rear emitter by means of 2D numerical simulation, in: Proceedings of the 25th EU PVSEC, Valencia, Spain, 2010 pp. 2280–2286.
[21] E. Sani, A. Toncelli, M. Tonelli, Spectroscopy of Ce-codoped Er:BaY2F8 single-crystals, Opt. Mater. 28 (2006) 1317–1320.
[22] P. Villars, BaY_2F_8 Crystal Structure, Material Phases Data System (MPDS) CH-6354 Vitznau, Switzerland, SpringerMaterials, sd_1411271 Springer-Verlag GmbH, Heidelberg, 2014.
[23] P. Villars, LYF4 Crystal Structure, Material Phases Data System (MPDS) CH-6354 Vitznau, Switzerland, SpringerMaterials, sd_1510118 Springer-Verlag GmbH, Heidelberg, 2014.
[24] H. Kühn, K. Petermann, G. Huber, Correction of reabsorption artifacts in fluorescence spectra by the pinhole method, Opt. Lett. 35 (2010) 1524–1526.
[25] M. Rüdiger, S. Fischer, J. Frank, A. Ivaturi, B.S. Richards, K.W. Krämer, M. Hermle, J.C. Goldschmidt, Bifacial n-type silicon solar cells for upconversion applications, Sol. Energy Mater. Sol. Cells 128 (2014) 57–68.
[26] H. Chou, H. P. Jenssen, Upconversion processes in Er-activated Solid State Materials, in: M. L. Shandand, H. P. Jenssen (Eds.), Proceedings of the Vol. 2 of the OSA Series Tunable Solid State Lasers, Optical Society of America Washington D.C., 1989, pp. 167–174.
[27] S. Ivanova, F. Pelle´, A. Tkachuk, M.F. Joubert, Y. Guyot, V.P. Gapontzev, Upconversion luminescence dynamics of Er-doped fluoride crystals for optical converters, J. Lumin. 128 (2008) 914–917.
[28] M.J. Weber, Selective excitation and decay of Er^{3+} fluorescence in LaF3, Phys. Rev. 156 (1967) 231.